Ground testing of the ETF unmanned airship technology demonstrator

P. Gili, M. Battipede, M. Vazzola
Aeronautical and Space Department, Politecnico di Torino – 10129 Torino, ITALY

P. Cassino
Nautilus s.p.a., 15076 Ovada, ITALY

ABSTRACT

This paper deals with the ground testing of the technological demonstrator of the innovative remotely controlled ETF airship[1]. The testing activities are intended to validate the flight control system of the ETF, which is based on the thrust vectoring technology and represents one of the major innovations of the ETF design, together with the airship architecture.
A research team of the Aeronautical and Space Department of the Polytechnic of Turin, in collaboration with Nautilus, a small Italian private company, has been working since a few years on the ETF (Elettra Twin Flyers). This airship is remotely-piloted, with high maneuverability capabilities and good operative features also in adverse atmospheric conditions[2].
The Nautilus new concept airship features architecture and appropriate command system, which should enable the vehicle to maneuver in forward, backward and sideward flight and hovering with any heading, both in normal and severe wind conditions. To achieve these capabilities the ETF demonstrator[3] has been conceived with a highly non conventional architecture based on a double hull with a central plane housing structure, propellers, on board electric system and payload (Figure 1). As primary command system, the aerodynamic control surfaces are replaced by six propellers, which are moved by electrical motors and allow the airship to be controlled and maneuvered in the whole flight envelope. In this paper the results of the preliminary testing runs are analyzed and the power requirement is compared with the performance of the Fuel Cell system, purposely developed for the ETF Demonstrator[4].

I Introduction

The low-cost multi-purpose multi-mission platform Elettra-Twin-Flyers (ETF) is being developed by the synergy of Nautilus S.p.A and the Politecnico di Torino [1]. It is a very innovative remotely-controlled airship equipped with high precision sensors and telecommunication devices. For its peculiar features, it is particularly suitable for inland, borderland and maritime surveillance missions as well as for telecommunication coverage extensions, especially in those areas which are either inaccessible or without conventional airport facilities and where the environmental impact is an essential concern.
ETF is characterized by great maneuverability as well as low wind sensitivity [2]. Flight conditions range from forward, backward and sideward flight to hovering, both in normal and severe wind conditions. To achieve these capabilities the ETF has been conceived with a highly non conventional architecture. The key point of the design is the innovative command system, which is completely based on thrust-vectoring propellers moved by electrical motors, powered by hydrogen fuel cells. The ETF concept comes from surveillance and monitoring purposes. The airship is designed to have great maneuverability to meet high level mission requirements, set to operate highly specialized instrumentation, such as light Synthetic Aperture Radar (SAR) systems or Electro-Optic (EO) infrared cameras or hyperpectral sensors. To fulfilling the average surveillance requirement, the system has a minimum endurance target of 48 hours with extension to 72 hours, with an altitude operation ranging from 500 to 1500 meters.

The ground tests are now in progress on the demonstrator [3], which is a reduced-scale reduced-complexity platform, purposely assembled to test the most critical subsystems, such as the command system and the architectural solution. During the feasibility study many aspects have been evaluated beyond the structural one. These aspects have been analyzed not only as independent problems, but also and especially for the impact they have on the structure and on the consequent choice of configuration. The comparison analyses have always been conducted in the respect of the control architecture geometry. The main constraint, in fact, is the control architecture which makes use of trust-vectoring propellers. It must be considered that, to some extent, the command strategy uniquely defines the number and position of the engines, according to the configuration of the demonstrator which is currently being tested (Figure 1 and 12).

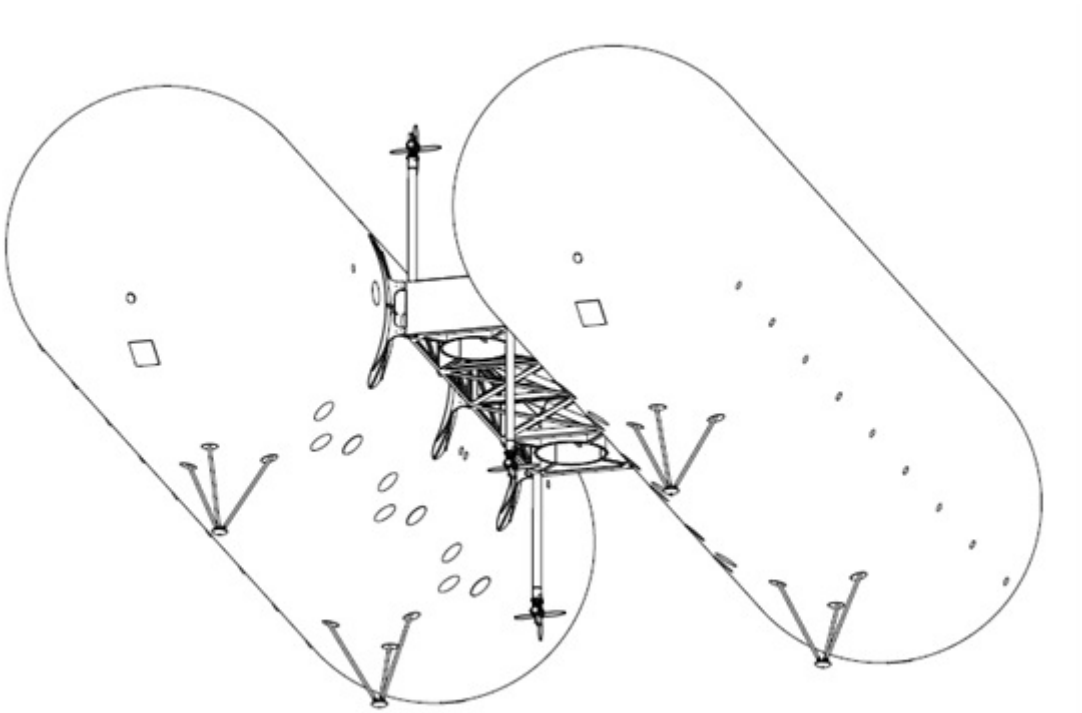

Figure 1 – ETF Demonstrator

As a consequence, the same constraint imposes load positions as well as weights for the auxiliary systems and for the onboard power unit.
As the platform is unmanned, however, it allows a simplified design since there are no constraints related to the ergonomics of the pilot and passenger compartment. The on-board systems are also greatly simplified and reduced. The considerable amount of volume available on the ETF has permitted the evaluation of different solutions for the energy storage, namely the storage of hydrogen necessary for the operation of fuel cells. In this context it is worth pointing out that it was the technological limitation imposed by the power generation that has generated the most stringent requirements for the architecture definition. These requirements may be translated into a twofold specification: on one side it is necessary to minimize the structural loads, converging to the lightest structure without reducing the amount of stored hydrogen, on the other side it is crucial to maximize the amount of hydrogen to provide competitive endurance.

II Control Technique

As introduced above, the ETF in characterized by an innovative control technique that is briefly explained hereinafter. The control procedure is carried on by the pilot action performed through an innovative cockpit, which will be described in details in the next section, consisting of two throttles and a three-DOF joystick. The pilot inputs are processed and re-allocated by the Control Allocation System, which is modeled in the *Flight Control Computer* (FCC), in order to generate the desired commands in terms of propeller rotational speeds and orientations of the four thrust-vectoring propellers. The control strategies within the FCC have been developed for the two possible flight conditions: forward flight and hovering with/without wind. In forward flight, the joystick commands the orientation δ of the four thrust-vectoring propellers for the lateral and directional maneuvers, as well as the differential variation of the angular rate of all the six propellers, generating the differential thrusts Δ_{Tax} and Δ_{TaxVT} for the longitudinal maneuvers. The allocation strategy of the longitudinal control, between forward and vertical propellers, has been purposely designed and scheduled to improve both the efficiency and the potentiality of this command, optimizing the airship performance in the whole speed range. Finally, the two throttle act on the collective rotational speed, respectively, of the four thrust-vectoring propellers and of the two vertical axis propellers. In particular, the variation Δn of the propeller rotational speed in revolutions per minute (RPM) is proportional to the square root of the throttle input δth. This relationship has been imposed to pursue a linear relation between the command action and the generated thrust when the propeller thrust is modeled through the first *Rénard formula* [5]:

$$T_{th} = \tau \rho_{air} \omega^2 R^4 \tag{1}$$

where R is the radius and ω is the angular rate of the propeller, whereas τ is the thrust coefficient, function of the propeller functioning point. All the propellers can work in reverse mode with reduce efficiency. The maximum collective thrust commanded by the throttle input δth is only a reduced percentage of the total available thrust, while the remaining available thrust is dedicated to the commanded maneuvers, which are thus always achievable even when the throttle command δth is maximum.

The general scheme of the control strategy in forward flight is illustrated in Figure 2, in which it is highlighted the position of each propeller with the corresponding control action generating positive pitching, rolling and yawing moments, respectively, for longitudinal, lateral and directional maneuvers.

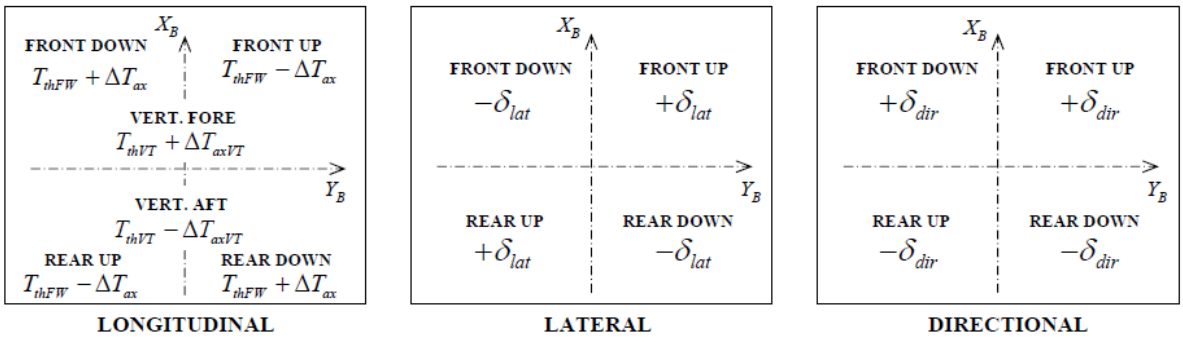

Figure 2 Control strategy in forward flight

The forward and vertical collective thrusts Tt_{hFW} and T_{thVT} are linearly controlled by the two throttles, while the differential thrusts ΔT_{ax} and ΔT_{axVT}, and the propeller orientations δ are generated through the joystick action. In particular, the joystick firstly commands the axial ΔT_{ax} and

normal ΔT_n thrust increments with respect to the propeller rotational axis, needed to accomplish the desired maneuvers. Successively, the FCC processes and re-allocates these signals in order to provide the corresponding orientation angles δ of the propellers in the lateral and directional maneuvers. Hence, it can be noticed that also the joystick inputs are proportional to the differential thrust components acting on the propellers.
The positive rotation δ of the thrust-vectoring propellers is assumed to be in a clockwise direction.
In hovering condition, the control strategy is analogous to the forward flight except that all the thrust vectoring propellers are collectively oriented in the wind direction through the angle δ_{coll}. In addition, differently from the forward flight, the directional command is accomplished through a differential thrust of the right and left forward propellers with respect to the longitudinal wind axis X_w. For the longitudinal and lateral maneuvers, the pilot continues to command the desired moments M_{yB} and M_{xB} in the body-axis reference frame through the inputs δ_{lonB} and δ_{latB}, while the FCC processes these commands and computes the corresponding control inputs in the wind axis reference frame. The relationship between the two sets of command inputs depends exclusively on the collective orientation angle δ_{coll} as shown by the following expression:

$$\begin{cases} \delta_{lon_w} = -\delta_{lat_B} \sin\delta_{coll} + \delta_{lon_B} \cos\delta_{coll} \\ \delta_{lat_w} = \delta_{lat_B} \cos\delta_{coll} + \delta_{lon_B} \sin\delta_{coll} \end{cases} \tag{2}$$

which is made possible since the joystick commands are proportional to the differential thrust of the propellers as assured previously. In this way, the hovering and forward flight conditions can be similarly treated by simply considering the collective orientation δ_{coll} of the four thrust-vectoring propellers in the wind direction.
This control allocation strategy is inherently based on two main assumptions. Firstly, the longitudinal thrust component, produced by the forward throttle δ_{th}, has to be preserved during any longitudinal, lateral and directional maneuver in order to guarantee the desired motion and speed of the airship. Secondly, the longitudinal and lateral commands either in forward flight or hovering have to be proportional to the related moments in order to pursue the relation expressed in Figure 3 by Equation (2). This control strategy can be summarized in Figure 4.

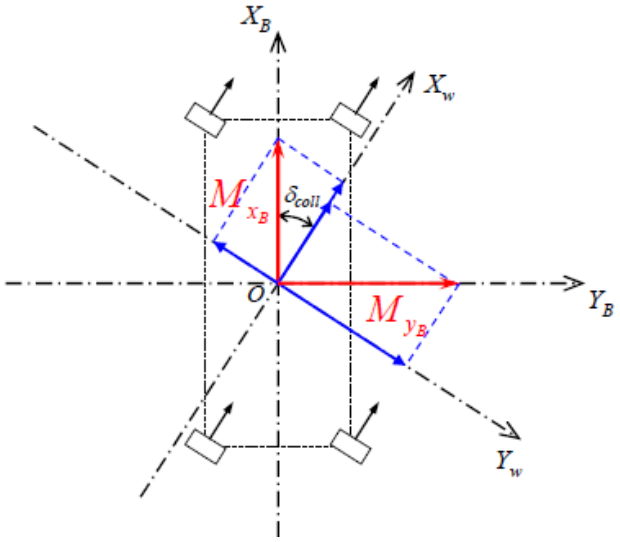

Figure 3: Hovering condition with wind

For example, when the pilot acts simultaneously on the longitudinal ($\delta_{lon} \propto \Delta T_{ax}$) and lateral/directional ($\delta_{comm} \propto \Delta T_n$) commands, the total commanded thrust can exceed its maximum value, that is $T \leq T_{\max}$

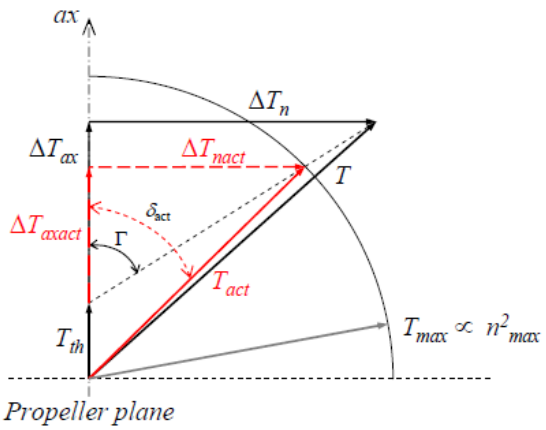

Figure 4 - Scheme of the command strategy

To avoid this drawback, the axial ΔT_{ax} and normal ΔT_n thrust increments have to be proportionally reduced for the second assumption above-mentioned at least up to ΔT_{axact} and ΔT_{nact} respectively, in order to generate a feasible thrust T_{act}, which will be equal to the maximum thrust $T_{\max}$. Initially, the FCC calculates the total commanded thrust for each propeller as:

$$T = \sqrt{\left(T_{th} + \Delta T_{ax}\right)^2 + \Delta T_n^2} \tag{3}$$

then, if max $T \leq T$ it places $T_{act} = T$ and estimates the feasible propeller orientation angle as:

$$\delta_{act} = \arccos\left(\frac{T_{th} + \Delta T_{ax}}{T}\right) \tag{4}$$

Otherwise, if max $T > T$ the FCC proportionally reduces the commanded thrust increments ΔT_{ax} and ΔT_n and computes the feasible propeller orientation angle as follows:

$$\begin{cases} T_{act} = T_{\max} \\ \delta_{act} = \arccos\left(\dfrac{T_{th} + \Delta T_{axact}}{T_{\max}}\right) = \arccos\left(\dfrac{T_{th} + \left[\sqrt{T_{\max}^2 + T_{th}^2\left(1 - \cos^2\Gamma\right)} - T_{th}\cos\Gamma\right]\cos\Gamma}{T_{\max}}\right) \end{cases} \tag{5}$$

where Γ is a geometric angle resulting from Figure 7 and Δ_{Taxact} can be expressed as function of T_{th}, $T_{\max}$ and Γ. As concerns the signs of T_{act} and δ_{act}, the thrust-vectoring propellers should be modeled to rotate within the range between -90° and +90° and use the reverse mode. This can be obtained by considering:

$$\begin{cases} sign\left(T_{act}\right) = sign\left(T_{th} + \Delta T_{ax}\right) \\ sign\left(\delta_{act}\right) = sign\left(\delta_{comm}\right) \cdot sign\left(T_{act}\right) \end{cases} \tag{6}$$

where δ_{comm} is the composition between lateral and directional commands.

III. Piloting modes

Currently almost all the manned and unnamed aircraft are flown by mean of a throttle, combined with a stick and pedals. This configuration has always been considered the best compromise between two counteracting requirements:

-simplify the mechanical connections between commands and actuators

-reduce the pilot workload pursuing ergonomics and piloting intuitiveness.

It is becoming quite evident, however, that throttles and stick are restrictive for the EFT airship and the effort of adapting a conventional cockpit to the ETF airship could reveal useless or even counterproductive.

For this reason, a new user interface is being developed to minimize the pilot workload and enhance the ETF airship peculiarities, especially in hovering and near-hovering conditions. A drastic reduction of the pilot workload is also beneficial to increase the global situation awareness and safety, as a consequence. The ETF is also capable of semiautonomous operations and the new interface must be able to handle high level commands, such as cursor-on-target path following on a GPS-referenced map.

The main component of the new interface is a commercial device, commonly named spacemouse, which is usually employed in the 3D CAD and CAE design and has proven to be particularly effective in reducing the discomforts associated to the handling of three-dimensional objects through a two-dimensional device, such as the monitor.

A single mobile component provides the user with the 6 degrees of freedom: it is hold with one hand and can be moved and rotated along the three axes. Common mice or trackballs work with two degrees of freedom and require auxiliary function keys or buttons. The difference is particularly evident when the control action requires fast and frequent accommodations.

The implementation is quite intuitive: it takes advantage of the spacemouse degrees of freedom, which are conceptually associated with the airship movements and rotations. Moving the spacemouse in the horizontal plane will cause the airship to move in the same plane, vertical displacements implie altitude variations whereas the three rotations control the ETF attitude. The transition between position and speed control is straightforward.

This strategy is being very effective in enhancing the airship peculiarities, maximizing handling and piloting qualities. The intuitiveness of this piloting technique proven to be also very helpful in reducing much of the stress associated with critical operations, such as takeoff and landing. The synchronized use of two hands to coordinate speed and attitude is no longer necessary. This innovative piloting technique, moreover, can be easily decontextualized and applied to other UAVs, which could be flown even by little specialized pilots.

Elattra-Twin-Flyer can be flown in three different modes. In the first mode the airship is guided manually and commands are sent continuously in form of percentage of the active effective. A Stability Augmentation System guarantees a fairly good maneuverability in the whole flight envelope. In the second mode a Control Augmentation System is coupled with the airship dynamics. Commands are still sent continuously from the ground station, but in form of desired linear and rotational speed values. In the third mode control is fully automated, such that an autopilot maintains flight control using preprogrammed fly-to coordinates. In the following subsections these three modes will be further discussed.

1. Remotely Piloting - In the remotely piloting mode, commands are generated by the pilot through an HOTAS system, consisting of two throttles and a three-DOF joystick. The pilot inputs are processed and re-allocated by the Control Allocation System implemented on the on-board Flight Control Computer (FCC), in order to generate the desired commands in terms of propeller rotational speeds and orientations of the four thrust-vectoring propellers. The control strategies within the FCC have been developed for the two possible flight conditions: forward flight and hovering with/without wind. In this condition the link is not

redundant because this control method should be used only during demo flights. The system is protected by the loss of datalink through an internal routine that ping the ground computer. As soon as the ping is lost a timer starts. If, before the counter reaches 10seconds, the ping returns available nothing happen, if not all the engine are stopped and the shut off valves are opened.

2. Semi-autonomous mode - In the Semi-autonomous mode the airship is interfaced to a Stability and Control Augmentation system (SCAS) which enable the pilot to command in terms of desired linear and rotational speed values. This is the mode where the spacemouse is particularly effective as the degrees of freedom can be directly associated to the relative speed commands. The SCAS is based on a set of Linear Quadratic Tracker (LQT) controllers correlated with one another through a Gain-Scheduling Interpolation. Since the airship model is inherently non-linear, in fact, different LQTs gains have been selected to cover the flight envelope, with steps on the speed absolute value as low as 1 m/s. In this condition a redundant link will be used to avoid loss of communication.

3. Autonomous mode - In the autonomous mode the airship is flown through a point-to-target procedure using preprogrammed fly-to coordinates. The pilot uses a very simple and intuitive Human Machine Interface (HMI) to impose a set of waypoints on a 3D map. The choice of these waypoints represent the first step of an iterative procedure which allows the system to select a path, which should be optimized, according to the airship dynamic features and the payload capabilities. It should also respect the constraints given by the ATM control while avoiding the threat areas. In this condition the link is not safety critical, because the path is planned in a pre flight phase.

IV. Power generation

As already mentioned, a crucial aspect in the ETF design is the substantial amount of the internal volume. This is useful for two reasons: it allows, first, a more distributed allocation of the onboard systems, thereby avoiding concentration of loads, second, the evaluation of different solutions for the hydrogen storage.
The hydrogen storage is troublesome in many applications [6]: hydrogen surely has a very favorable energy density, in fact, but the ratio volume per unit of energy becomes comparable with more conventional fuels only if it is stored in high pressure tanks. This is crucial in certain applications, such as in the automotive or aerospace field, where the volume of fuel must be limited to maximize the payload capabilities. Moreover, it is clear that the presence of a high pressure tank can be considered an additional element in the fulfillment of the safety requirements. This is particularly evident for the automotive market, for example, where the tank must be designed to resist not only to the internal pressure, but also to the impact loads generated by a crush. The latter requirement is by far the more stringent for storage pressure lower than 200 atm. This means that even if there is an extra availability of volume, there is no convenience to store the hydrogen at pressure values lower than 200 atm. This consideration might partially solve the problem of the energy density (namely volume per unit of energy). On the other hand, what still needs to be increased is the ratio of energy stored on total weight, where total stands for fuel and container: for hydrogen fuel cells, in fact, it is currently about 0.75 kWh / kg. This value might be acceptable in the automotive applications, but in the aerospace field the requirements are more stringent, especially for high endurance vehicles.
For the specific case of the ETF, the board fuel volume is not an important constraint, whereas the reduction of the total weight is obviously critical, as in every aeronautical application. This is the reason why an alternative storage technology is being considered [4]. Among the other options, the huge available volumes suggest the gaseous hydrogen could be easily and safely stored in low-pressure light-weight tanks, which could be embedded in the helium envelopes.

This expedient could be very effective to diluted potential hydrogen losses, reducing the risk associated to a highly explosive gas. In this context, the technology is still not very developed, given the limited industrial interest. In order to investigate the possibility of adopting this solution for the ETF, a test bed has been assembled to test fuel cells fed with hydrogen at atmospheric pressure. The main problem is constituted by the compressor, which should be used to supply the fuel cell with a specific operative pressure, compressing the gas stored at atmospheric pressure. The employment of a compressor is uncommon in fuel cell systems, because usually the hydrogen is withdrawn by high pressure tanks (200-600 bar) and the pressure is then reduced in accordance to the anode specifications.
This technology, applied to the ETF prototype, could lead to a reduction of several hundred kilograms: for the ETF: it has been estimated, in fact, that the high pressure tank weight would be alone more than 80% of the weight of the whole fuel cell supply system. The low-pressure light-weight tank solution could be very effective in reducing weights and dangerous concentrate loads on the structure. It must be considered, however, that the hydrogen stored at atmospheric pressure produces extra buoyancy which must be balanced with ballast. To this purpose, water could be safely used. It could be stored in tanks and vaporized at a specific rate to equilibrate the loss of buoyancy due to the hydrogen consumption.
Within a parallel project conducted by the Polytechnic of Turin on a piloted aircraft, a 19 kW fuel cell power system has been designed. The same stack is being considered for the EFT main power source, as an alternative to the conventional batteries. This is thus the stuck used as a reference for the backup system described in the previous section.
The use of a Proton Exchange Membrane Fuel Cell (PEMFC) has been preferred for the high specific power to weight ratio, low operating temperature and high efficiency. Due to the high power demand and the high power over weight requirement, an active liquid cooling system has been chosen. To obtain high performance, hydrogen and air flows feed the stack with a pressure regulated up to 2 bars. The pressure levels are proportional to the fuel cell power output, but an extra pressure regulation is also necessary to balance the differential actions on the two faces of the stack membranes with the flight altitude.
In addition to the 19kW stack, a backup system composed of super capacitor is needed in order to supply the peak power demand needed during acceleration. To choose the size of this backup system an analysis of the actual power peaks is needed in order to avoid an excessive over dimensioning that will cost a lot in terms of weight.

V Ground Tests - Power demand

The above energetic system is dimensioned in order to guarantee the nominal power needed by the main engines during forward flight. Another component has to be dimensioned: the auxiliary capacitors.
The control system of the ETF requires high precision in the control of individual electric motors, thus requiring a sophisticate actuation system that need peaks of power to maneuver. In addition, the engines must first meet the power and weight requirements. The entire command line consists of three elements: first we have the control board, which is the interface that connects to the control system, then the engine itself, and finally an encoder, which is a tool that converts speed or position of a rotating system into an analog or digital signal. The encoder is required to allow the board to operate according to a closed loop scheme and continually checking that the motor is actually running at the required speed. The control board must be able to provide the motor with the appropriate voltage and current in order to control the rotational speed. It was decided that the communication interface was a serial RS-422, since it allows great freedom with regard to the communication protocols and is relatively simple to implement, compared, for example, to a more complex interface such as a CAN-bus . The board must of course meet the appropriate criteria of

lightness, impermeability and resistance to weather conditions. The choice fell on a custom board developed in collaboration with Akse s.r.l..
Also the electric motor have been developed starting from a standard model, the Motorpower Tetra 100SR9.5. The customization regarded the bearings system and the flange. Those components were modified for structural reasons. The flange needed an adaptation to be compatible with the propeller's hub and the bearing system was adapted to fulfill the torque and trust requirements. Normally the engine are designed to resist to an axial loads equal to the maximum torque, in this case also the propeller gyroscopic effects and the propeller trust had to be taken into account during the bearings definition. This is a DC brushless motor, weighing about 4 kg, capable of a maximum continuous torque of 8Nm @ 6000 RPM.
The last component is the encoder, which must be incremental and compatible with the requirements of the control. The encoder is required because without it, the card would work in an open loop scheme, without any assurance that the actual speed reached is the right one. Working in closed-loop, the card has a feedback on the actual motor speed and thus can vary the torque to guarantee the consistency of the command.
To make an assessment on the required power, a test bench has been built. The test bench consists of the hardware described above, plus the power supplier and the actual propeller. This type of test bench can assess the real power absorption during both acceleration and steady state.
The test bench was instrumented with current and voltage probes in order to register the power that flows through the wires. An indirect readout of the torque has been performed starting from the power divided by the rotational speed expressed in *rad/sec*.
The propeller torque and power curves are shown in figures 5 and 6.

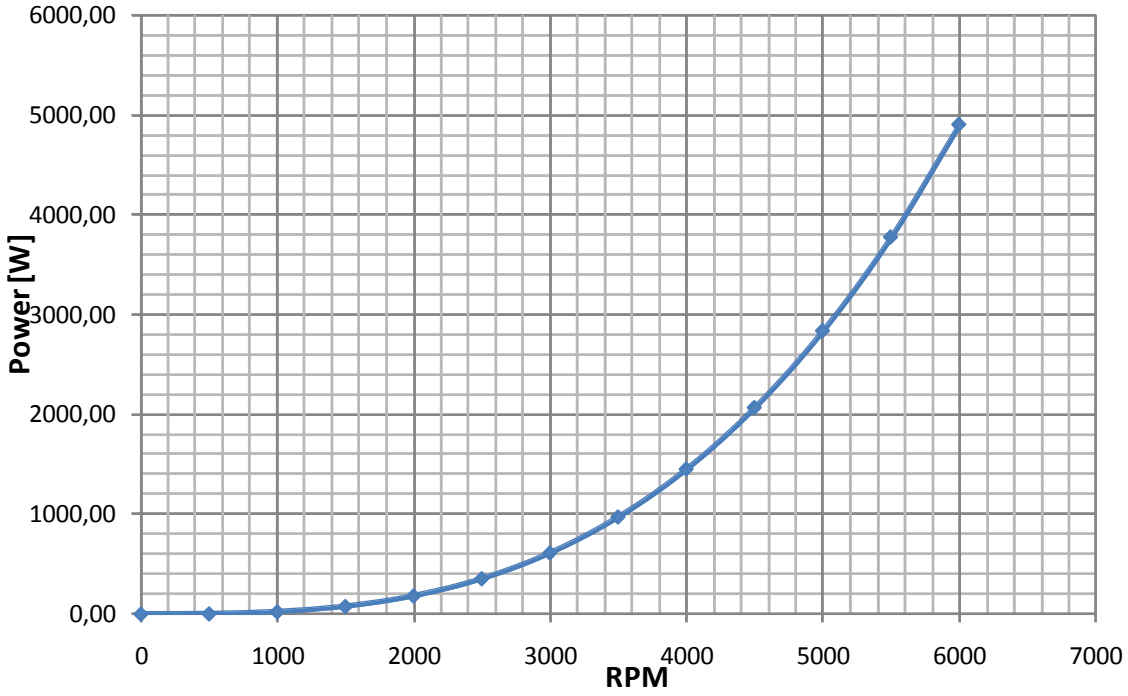

Figure 5 - Propeller power requirement

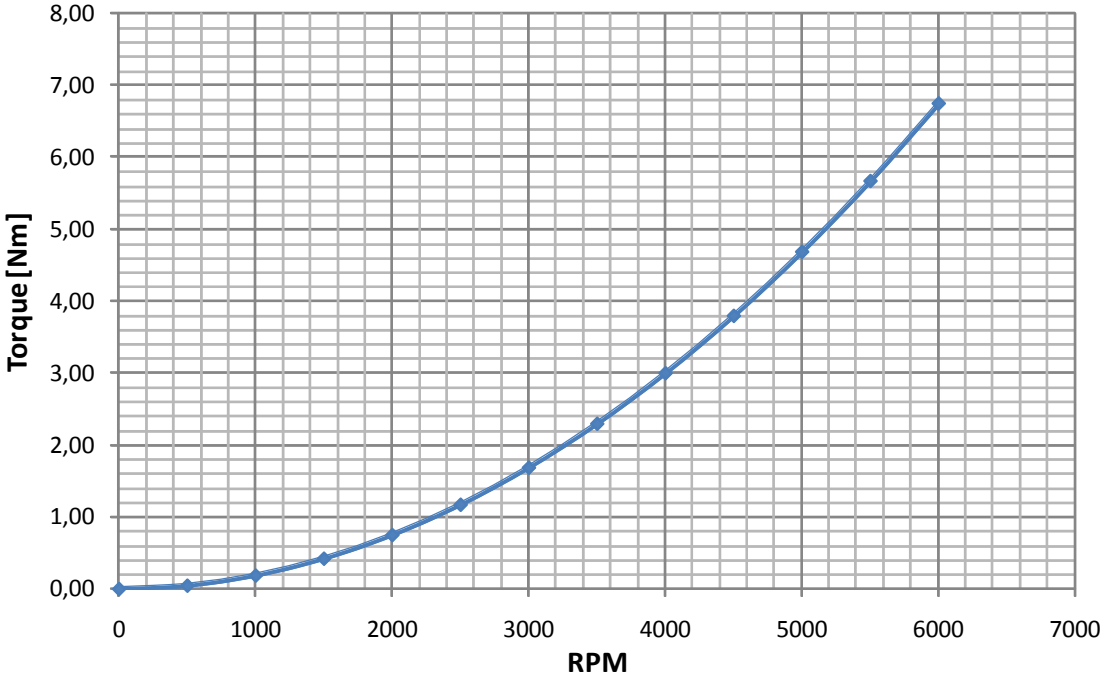

Figure 6 - Propeller torque requirement

To determine the requirements of the engines, it was analyzed the torque and power required as a function of the forward speed and of the rotational speed, or, more precisely, as a function of γ, which is the advance ratio of the propeller V/ωR, where V is the speed, ω the rotational speed and R the radius of the propeller. Torque and thrust can be referred to the torque and thrust coefficients κ e τ as follows:

$$C = k\rho\omega^2 R_e^5 \qquad T = \tau\rho\omega^2 R_e^4 ; \tag{7}$$

where κ e τ are defined on the basis of propeller characteristics (figure 7).

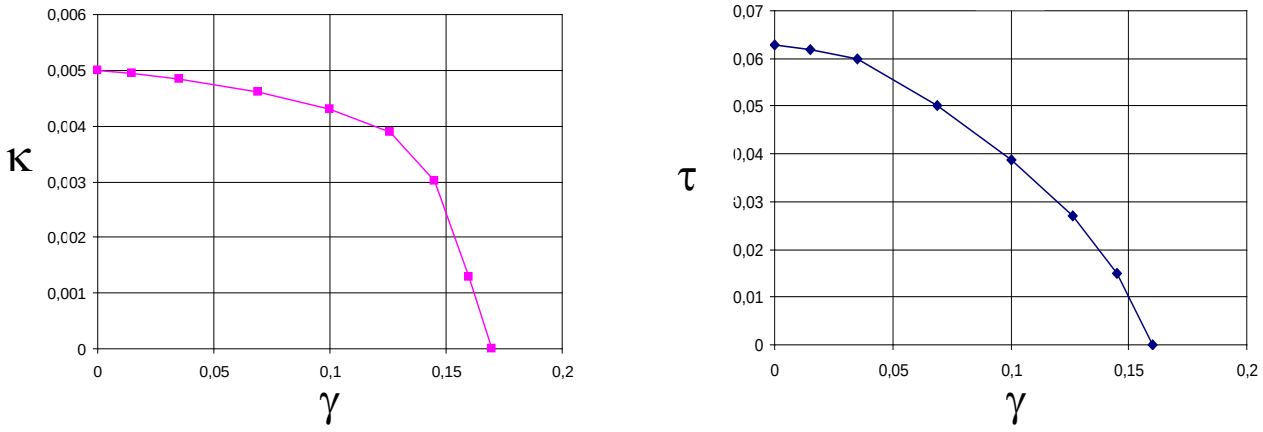

Figure7: k and τ diagrams function of γ

The power and torque curves of figures 8 and 9 are then plotted by assuming some values of V and ω accordingly, and by calculating C and T from equation 7 through k and τ obtained from figure 7.

The calculated points define the performance points that, joined together, define the propeller operating curves. Power and torque of figure 8 and 9 are hence parameterized with the rotational speed of the propellers, and traced as a function of speed.
Two types of operations have to be defined, the regime operation and the maneuvering operation that correspond to different curves. Since the commanded speed is limited by the control system to ensure maneuverability even in maximum speed conditions, the requirements in the regime operation conditions are not particularly high. They just represent the limits of use that the engine has to ensure for long periods. Note that the curve in steady state is cut beyond 15 m/s, as this is the maximum speed reached by the ETF horizontally (this corresponds to a propeller rotational speed of about 320 rad/s).

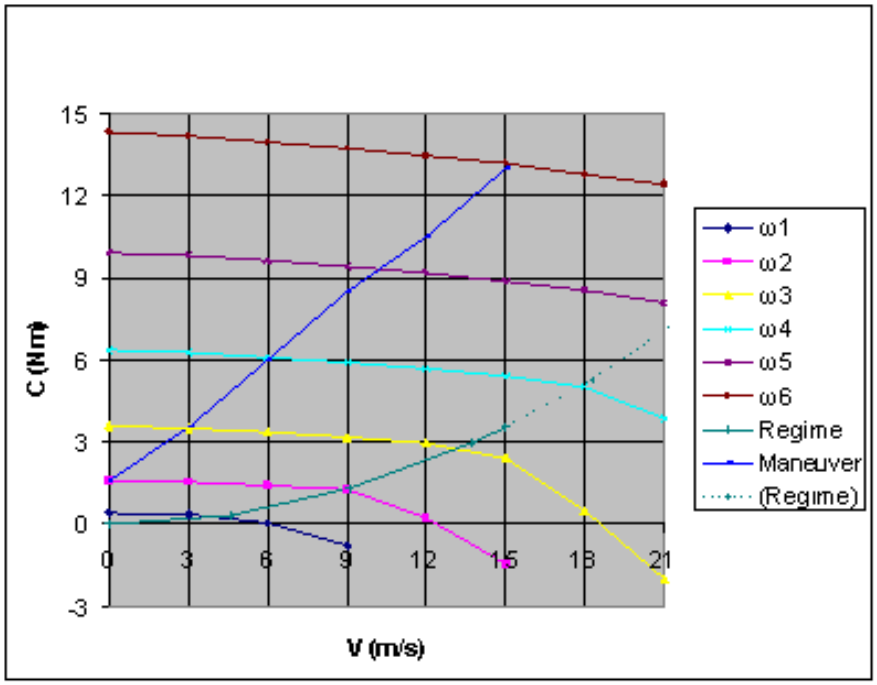

Figure 8 – Torque requirement versus forward speed

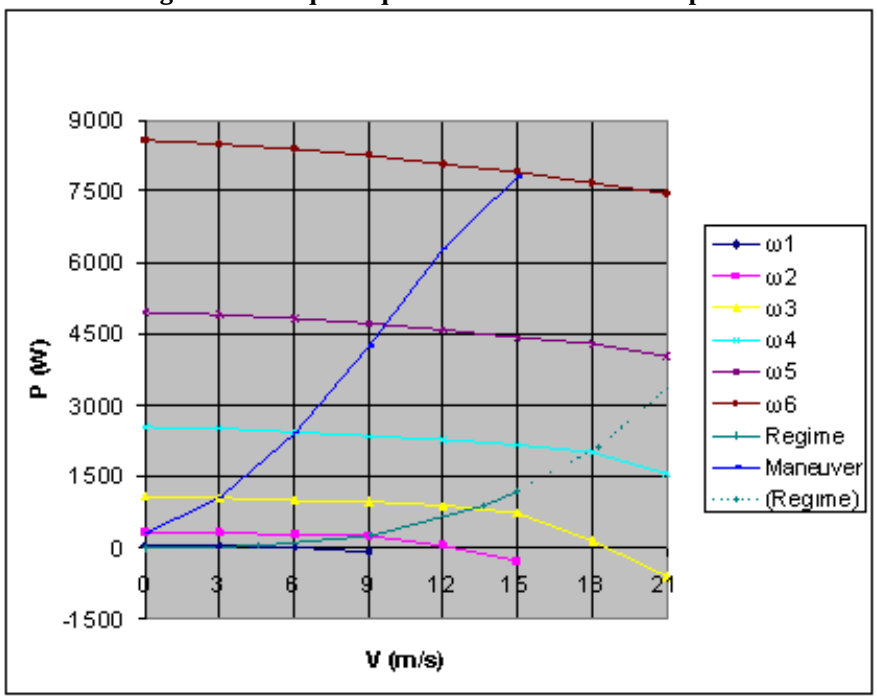

Figure 9 – Power requirement versus forward speed

After the definition of the power and torque curves, the average energy required to perform a standard mission can be estimated. In particular, the instant power can be calculated simulating the overall mission on the flight simulator. A mission profile example is shown in figure 10, whereas figure 11 shows the propellers rotational speed for the first 120 seconds of the mission.

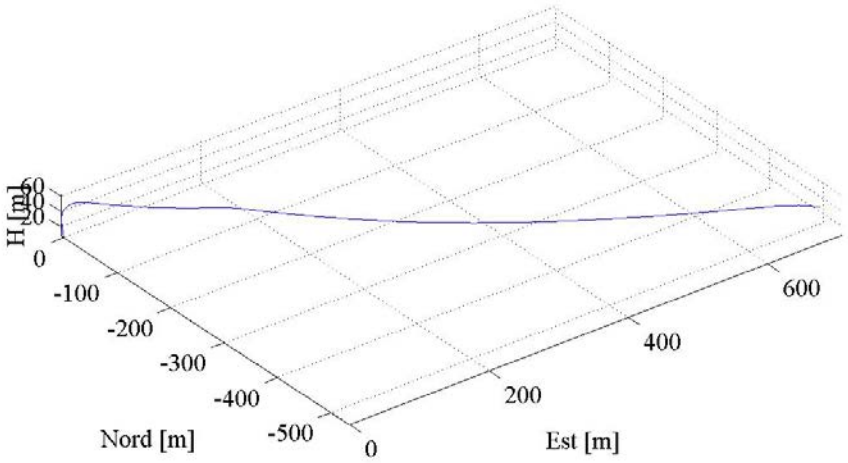

Figure 10 - Mission profile – manouvered forward flight

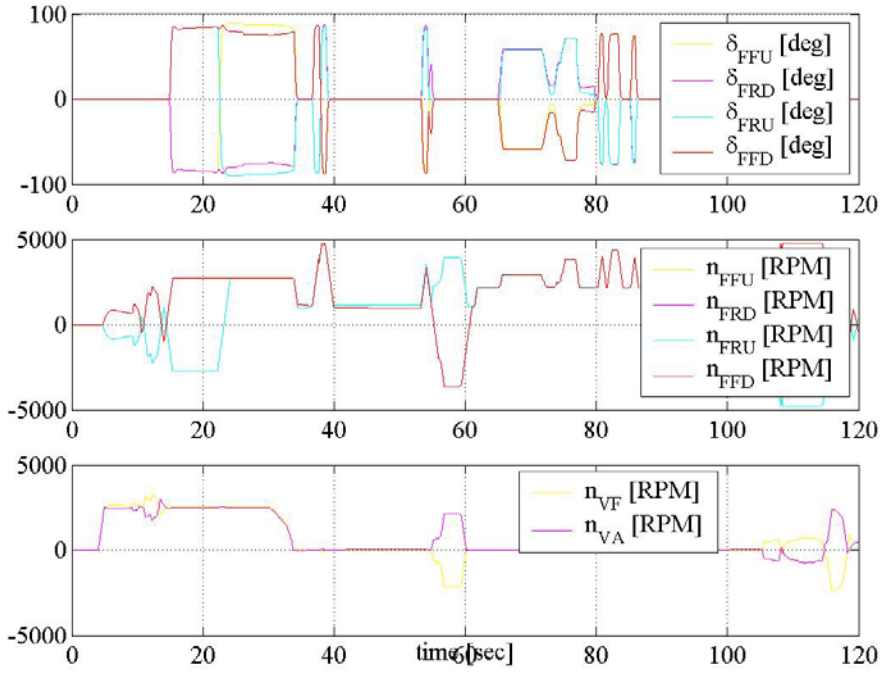

Figure 11 - Engine data (orientation – forward rotational data – vertical rotational data)

VI Conclusions

These tests show that the energetic system defined in section 3 allow us to perform the demonstrational flight. A 10kW super capacitor system can guarantee a good compensation between the fuel cell power and the peaks calculated in the above section. Moreover, while this type of mission has a low endurance and low thrust requirements, the energy stored in 1kg of hydrogen can be enough to fulfill the energy consumption calculated during the ground tests. 15 minutes is the time needed to test all the flight capabilities of the ETF demonstrator such as the roll, pitch yaw capability and to perform a fly by on the testing area. After these maneuvers the hydrogen left in the

tank is enough for a safe landing inside the target area. This final landing, with adverse wind, is one of the key of the flight demonstration, in order to show the maneuvering capabilities of the ETF. The ETF heading can be decided by the pilot and the propellers guarantee the controllability during all the test phases. Last but not least there is the system weight assessment. The three main component of this system, in terms of weight, can be obviously identified in the fuel cell, the super capacitor and the hydrogen tank. The fuel cell has been already used and its weight is 30kg, including 10kg of stack. The super capacitor, needed to guarantee the power peaks requested during maneuvering, assuming 1 minute of peak, weights 30kg [7]. The third component, the hydrogen tank, is the smallest in terms of weight, in fact to store 1kg of hydrogen only 20kg are needed. This leads to a total system weight of 80kg in order to perform the desired demonstration.

Figure 12 – ETF Demostratore in the Hangar @ Reggio Emilia

[1]Inventors: Gili, P.A., Battipede, M., Icardi, U., Ruotolo, R., Vercesi, P., Owner: Nautilus S.p.A. and Politecnico di Torino, "Dual hull airship controlled by thrust vectoring," N. PCT/EP03/08950, August 2003.

[2]Battipede, M., Lando, M., Gili, P.A., Vercesi, P., "Peculiar Performance of a New Lighter-Than-Air Platform for Monitoring", Proceedings of the AIAA Aviation Technology , Integration and Operation Forum, AIAA, Reston, VA, 2004.

[3]Battipede, M., Gili, P.A., Lando, M., "Prototype Assembling of the Nautilus Remotely-Piloted Lighter-Than-Air Platform", Proceedings of the AIAA Aviation Technology , Integration and Operation Forum, AIAA, Reston, VA, 2005.

[4]Battipede, M., Gili, P.A., Vazzola, M., "Innovative Hydrogen Storage Tank for Flying Fuel Cell Power System", Proceedings of the AIAA 6th International Energy Conversion Engineering Conference (IECEC) Cleveland, Ohio – July 28-30, 2008.

[5]Lausetti, A., Filippi, F., *Elementi di Meccanica del Volo*, Vol. 1, ed. Levrotto & Bella, Turin, 1955, pp. 61-88.

[6]Mitlitsky, F., Weisberg, A.H., and Myers B., "Vehicular hydrogen storage using lightweight tanks", Proceedings of the 2000 U.S. DOE Hydrogen Program Review NREL/CP-570-28890, May 1999.

[7]Ying Wu, Hongwei G., "Optimization of Fuel Cell and Supercapacitor for Fuel-Cell Electric Vehicles", IEEE Transactions on vehicular technology, vol. 55, no. 6, November 2006